Medicinal chemistry

Mejai et al., Med Chem (Los Angeles) 2018, 8:4
DOI: 10.4172/2161-0444.1000497

Research Article Open Access

Synthesis and Evaluation of Antiplasmodial Activities of Fluorinated 6-Amino-2-Aryl-3H-Indolone-*N*-Oxides

Amani Mejai[1]*, Ennaji Najahi[1,2], Gneigny Tchani[3], Pierre Perio[2], Laure Vendier[4,5], Sandra Bourgeade Delmas[2], Rym Abidi[1], Mohamed Haddad[2], Françoise Nepveu[2#] and Karine Reybier[2#]

[1]*Faculté des Sciences de Bizerte, LACReSNE, Interactions Moléculaires Spécifiques, Université de Carthage, Zarzouna-Bizerte, Tunis TN 7021, Tunisie*

[2]*Pharmadev, UMR 152, Université de Toulouse, IRD, UPS, France*

[3]*Faculté des Sciences, Université de Lomé, BP 1515, Lomé, Togo*

[4]*LCC, Laboratoire de Chimie de Coordination, CNRS, Toulouse, France*

[5]*Université de Toulouse, UPS, INPT, LCC, F-31077 Toulouse, France*

[#]*These authors contributed equally to the work*

Abstract

A series of novel 6-amino-2-aryl-3*H*-indolone-*N*-oxides were synthesized at yields of up to 65% and characterized; one was further characterized using X-ray crystallographic analysis. Synthesized compounds were evaluated for their *in vitro* activity against a chloroquine-resistant (FcB1) strain of *Plasmodium falciparum*, as well as for the 50% cytotoxic concentration (CC_{50}) on Vero cell lines. The most promising activities were observed for the fluorinated compounds, the most active *in vitro* being 6-(2-morpholinoacetamido)-2-(4-(trifluoromethoxy) phenyl)-3*H*-indolone-*N*-oxide (IC_{50}: 15.5 nM). In addition, these compounds showed weak cytotoxicity leading to selectivity index values of >170, thus warranting further *in vitro* and *in vivo* studies.

Keywords: Synthesis; Fluorinated indolone-*N*-oxides; Antiplasmodial activity; Cytotoxic activity

Introduction

Many organofluorine compounds have been approved by the US Food and Drug Administration (FDA) for medical use, which clearly demonstrates the importance of fluorine in medicinal chemistry [1-4]; some of these compounds have shown particular efficacy as antimalarial agents (such as mefloquine hydrochloride) (Figure 1). In the design and development of biologically active compounds, substitution of fluorine for hydrogen and hydroxy group often introduces beneficial properties such as good lipophilicity, metabolic stability, increased binding to target molecules and membrane permeability [5-7].

Over the past few years, we have designed and synthesized a series of 2-aryl-3*H*-indolone-*N*-oxides (INODs) (Figure 1) that has antiplasmodial properties targeting the asexual blood stage of *Plasmodium falciparum*, with IC_{50} values in the 1 to 100 nM range [8]. In addition to being active at nM concentrations, these compounds have non-toxic and non-hemolytic properties in healthy and parasitized erythrocytes [8] and are bioreducible [9]. The preparation of a large panel of compounds with different oxidation states [10] showed that only the compounds displaying the reducible N=C bond together with a pseudo-quinoid structure were active.

The bioreduction of these INODs produces free radicals [11-13]. With further studies on parasitized red blood cells (RBCs), we showed that these free radicals activate a SYK kinase cascade, which induces hyper-phosphorylation of the major protein in RBCs, band 3 anion transport protein [14], which, in the case of parasitized RBCs, causes an oxidative burst that is fatal to the parasite. We have recently shown that the anti-malarial activity of INODs was linked to their ability to serve as quinone reductase 2 substrates [13]. However, these molecules present two disadvantages: a poor water solubility and a rapid metabolization. To overcome their low aqueous solubility *in vivo*, INODs were formulated as albumin-based nanoparticles, and these strongly inhibited parasitemia in a mouse model infected with *Plasmodium berghei* (99.1% inhibition) or in humanized mice parasitized with *P. falciparum* (99.6% inhibition) [15]. Although the strong antimalarial activities have been shown *in vivo*, the solubility and metabolic stability of these compounds needs to be improved.

Successive structural modifications showed that the groups R^1 or R^2 at the 5- or 6-position had no major effect on the activity, whereas variation of R^3 at the para-position of the aryl group allowed for the most promising activities. The inclusion of a chloro group at the R^3 para-position provided the most active compound *in vivo* (Figure 1, Lead 1). On the other hand, introduction of the dimethylamino group at this position gave the most active compound *in vitro* (Figure 1, Hit 1); it had better water solubility and good antiplasmodial activity *in vitro* (CI_{50}<3 nM with the chloroquine-resistant FcB1 strain of *P. falciparum*) but poor inhibition of parasitemia *in vivo* (15.3%) (Figure 1). We therefore synthesized new fluorinated INODs with morpholino or piperidine groups in the C-6 position of the INOD scaffold to obtain better water solubility while keeping the antiplasmodial activity. The amino groups were linked to different fluorinated INODs via ether, ester or amide linkage.

We evaluated our series of novel fluorinated 6-amino-indolone-*N*-oxides (Figure 1) for their antimalarial activity against *P. falciparum* FcB1.

Materials and Methods

Chemistry

Reagents and solvents obtained from commercial suppliers were

***Corresponding author:** Amani Mejai, Faculté des Sciences de Bizerte, LACReSNE, Interactions Moléculaires Spécifiques, Université de Carthage, Zarzouna-Bizerte, Tunis TN 7021, Tunisie, Tel: 0021698585828; E-mail: ameni.mejai@gmail.com

Received March 06, 2018; **Accepted** March 09, 2018; **Published** April 11, 2018

Citation: Mejai A, Najahi E, Tchani G, Perio P, Vendier L, et al. (2018) Synthesis and Evaluation of Antiplasmodial Activities of Fluorinated 6-Amino-2-Aryl-3H-Indolone-N-Oxides. Med Chem (Los Angeles) 8: 079-085. doi: 10.4172/2161-0444.1000497

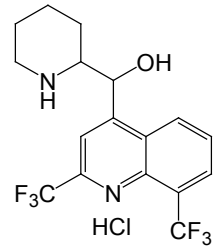

Mefloquine hydrochloride

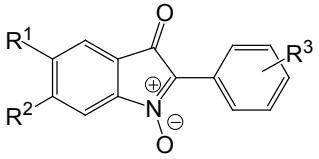

Indolone-*N*-oxides

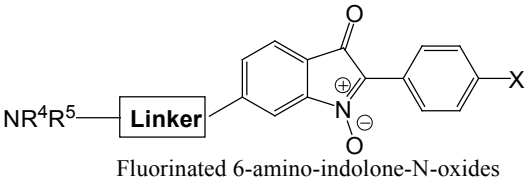

Fluorinated 6-amino-indolone-N-oxides

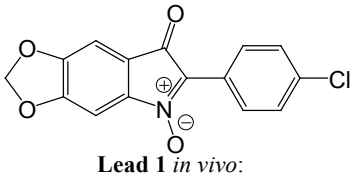

Lead 1 *in vivo*:

IC_{50}, nM (FcB1; 3D7): 75 ± 63; 58 ± 17.

CC_{50}, µM (MCF7; KB): 15.9; 27.

SI (MCF7/FcB1); (KB/3D7): 212; 450.

$t_{1/2}$ (mouse and human liver microsomes) < 1 min.

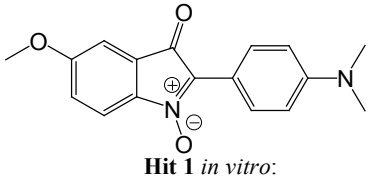

Hit 1 *in vitro*:

IC_{50}, nM (FcB1; 3D7): < 3; 1.7.

CC_{50}, µM (MCF7; KB): 43.9; 338.

SI (MCF7/FcB1); (KB/3D7): > 14 623; 198 823.

Figure 1: Structure of mefloquine hydrochloride and indolone-N-oxides.

used without further purification. Melting points were determined with an Electrothermal 9300 capillary melting point apparatus and are uncorrected. IR spectra were recorded on a Perkin-Elmer PARAGON 1000 FT-IR spectrometer. ^{1}H and ^{13}C NMR spectra were recorded on an AC Bruker spectrometer at 300 MHz (^{1}H) and 75 MHz (^{13}C) using $(CD_3)_2SO$ and $CDCl_3$ as solvents. HRMS were recorded on a Thermofisher scientific LTQ-Orbitrap-XL-ETD spectrometer (PHARMA-*DEV*, Toulouse, France). Silica Gel 60 (Merck 70-230) was used for column chromatography. All reactions were monitored by TLC aluminum/silica gel plate with UV-light visualization. Compound purity was determined by HPLC-UV and LC-PDA-MS methods and was ranged 96-99%.

Synthesis

Synthesis of o-iodonitroaryls c-i: See Supporting Information.

General procedure for the preparation of 6-(2-amino(ethoxy, acetamido or acetoxy)-2-arylindolone-N-oxides 9-20: $Pd(PPh_3)_2Cl_2$ (0.1 mmol) was added to a solution of a commercial alkyne (1 mmol) and 2-iodonitroaryl **c-i** (1 mmol) in freshly distilled triethylamine (20 mL) and DMF (10 mL), and the mixture was de-aerated with argon for 30 min. CuI (0.05 mmol) was added, and the mixture was de-aerated with argon for 10 min and stirred at room temperature for 6 h. The solution was then diluted with ethyl acetate (50 mL) and washed with water (3 × 50 mL). The organic phase was separated, washed with brine, dried over Na_2SO_4, and solvents were evaporated under reduced pressure. The residue obtained was added to a solution of $Pd(CH_3CN)_2Cl_2$ (0.05 mmol) in CH_3CN (15 mL), and the mixture was refluxed for 3 h in an argon atmosphere. The reaction mixture was concentrated, and the residue obtained was purified by column chromatography (ethyl acetate in petroleum ether).

***2-(4-Fluorophenyl)-6-(2-morpholinoethoxy)-3-oxo-3H-indole-1-oxide 9*:** Orange solid, yield: 82%, mp: 128-130°C. ^{1}H NMR (300 MHz, $CDCl_3$): δ: 8.81-8.74 (m, 2H), 7.57 (dd, *J*=8.2, 0.3 Hz, 1H), 7.28 (d, *J*=1.9 Hz, 1H), 7.24-7.16 (m, 2H), 6.96 (dd, *J*=8.2, 2.2 Hz, 1H), 4.27 (t, *J*=5.6 Hz, 2H), 3.78- 3.73 (m, 4H), 2.87 (t, *J*=5.6 Hz, 2H), 2.63-2.60 (m, 4H). ^{13}C NMR (70 MHz, $CDCl_3$): δ: 185.7, 164.8, 162.0, 150.5, 131.9, 130.4 (2C), 130.3 (2C), 123.6, 122.4, 115.9, 115.1, 101.9, 67.2, 66.9 (2C), 57.2, 54.1 (2C). IR (KBr, cm^{-1}): 1702, 1643, 1600, 1526, 1499, 1378, 1229, 1166, 1114, 1071, 1004, 850. MS-(+ESI), *m/z*: 371 $[M + H]^+$, 411, 449. ESI-HRMS $[M + H]^+$ calcd. for $C_{20}H_{20}FN_2O_4$: 371.1402, found: 371.1414.

***6-(2-Morpholinoethoxy)-3-oxo-2-(4-(trifluoromethoxy)phenyl)-3H-indole 10 1-oxide*:** Orange solid, yield 82%, mp: 124-126°C. ^{1}H NMR (300 MHz, $CDCl_3$): δ: 8.81-8.76 (m, 2H), 7.59 (d, *J*=8.2 Hz, 1H), 7.35 (ddt, *J*=8.1, 2.1, 1.0 Hz, 2H), 7.29 (d, *J*=2.1 Hz, 1H), 6.98 (dd, *J*=8.2, 2.2 Hz, 1H), 4.28 (t, *J*=5.6 Hz, 2H), 3.78- 3.75 (m, 4H), 2.88 (t, *J*=5.6 Hz, 2H), 2.63-2.60 (m, 4H). ^{13}C NMR (70 MHz, $CDCl_3$): δ: 185.5, 164.8, 150.3, 129.8, 129.7 (2C), 124.5, 123.7, 122.1, 120.5 (2C), 118.6, 116.0, 115.1, 102.0, 67.2, 66.9 (2C), 57.2, 54.1 (2C). IR (KBr, cm^{-1}): 1715, 1593, 1526, 1499, 1456, 1375, 1252, 1200, 1115, 846. MS-(+ESI), *m/z*: 437 $[M + H]^+$. ESI-HRMS $[M + H]^+$ calcd. for $C_{21}H_{20}F_3N_2O_5$: 437.1319, found: 437.1330.

***2-(4-Fluorophenyl)-6-(2-morpholinoacetoxy)-3-oxo-3H-indole 1-oxide 11*:** Red solid, yield: 45%, mp: 229-231°C. ^{1}H NMR (300 MHz, C_3D_6O): δ: 8.81-8.74 (m, 2H), 7.53 (dd, *J*=8.0, 0.3 Hz, 1H), 7.36-7.24 (m, 2H), 7.14 (dd, *J*=2.1, 0.4 Hz, 1H), 7.01 (dd, *J*=8.0, 2.1 Hz, 1H), 3.84-3.81 (m, 4H), 3.04 (s, 2H), 2.69 - 2.66 (m, 4H). ^{13}C NMR (70 MHz, C_3D_6O): δ: 185.3, 167.9, 164.0, 161.6, 150.9, 131.2, 130.1 (2 C), 123.6, 123.2, 116.5, 115.2 (2 C), 114.2, 102.4, 66.5 (2 C), 59.3, 53.1 (2 C). IR (KBr, cm^{-1}): 3406, 1703, 1649, 1592, 1525, 1497, 1479, 1371, 1254, 1160, 1059, 844. MS-(-APCI), *m/z*: 256 $[M - C_6H_{10}NO_2]^-$. ESI-HRMS $[M - C_6H_{10}NO_2 + H]^+$ calcd. for $C_{14}H_9FNO_3$: 258.0561, found: 258.0566.

***6-(2-Morpholinoacetoxy)-3-oxo-2-(4-(trifluoromethoxy)phenyl)-3H-indole 1-oxide 12*:** Red solid, yield: 64%, mp: 218-220°C. ^{1}H NMR (300 MHz, C_3D_6O): δ: 8.81-8.76 (m, 2H), 7.58 (d, *J*=8.2 Hz, 1H), 7.35-7.32 (m, 2H), 7.29 (d, *J*=2.1 Hz, 1H), 6.98 (dd, *J*=8.2, 2.2 Hz, 1H),

3.85-3.83 (m, 4H), 3.04 (s, 2H), 2.69-2.65 (m, 4H). ^{13}C NMR (70 MHz, C_3D_6O): δ: 185.5, 168.1, 161.7, 152.6, 129.8, 129.7 (2C), 124.5, 123.7, 122.1, 120.5 (2C), 118.5, 115.9, 115.1, 102.0, 66.8 (2 C), 58.1, 54.4 (2 C). IR (KBr, cm^{-1}): 3434, 1704, 1685, 1653, 1580, 1523, 1376, 1252, 1181, 1093, 1010, 845. MS-(-APCI), *m/z*: 322 [M - $C_6H_{10}NO_2$]$^{-}$. ESI-HRMS [M - $C_6H_{10}NO_2$ + H]$^+$ calcd. for $C_{15}H_9F_3NO_4$: 324.0478, found: 324.0483.

2-(4-Fluorophenyl)-6-(2-morpholinoacetamido)-3-oxo-3H-indole 1-oxide 1: Orange solid, yield: 48%), mp: 103-104°C. ^{1}H NMR (300 MHz, $CDCl_3$): δ: 9.56 (s, 1H, NH), 8.80-8.73 (m, 2H), 7.88-7.84 (m, 2H), 7.61 (dd, *J*=7.9, 0.5 Hz, 1H), 7.24-7.16 (m, 2H), 3.84-3.81 (m, 4H), 3.22 (s, 2H), 2.69-2.66 (m, 4H). ^{13}C NMR (70 MHz, $CDCl_3$): δ: 185.7, 168.5, 165.4, 162.0, 149.4, 143.7, 130.4 (2 C), 123.2, 122.3, 120.0, 117.8, 115.7 (2 C), 105.5, 67.0 (2 C), 62.4, 53.8 (2 C). IR (KBr, cm^{-1}): 3414, 3295, 1705, 1643, 1512, 1422, 1374, 1250, 1114, 1067, 846. MS-(+ESI), *m/z*: 384 [M + H]$^+$, 767 [2M + H]$^+$. ESI-HRMS [M + H]$^+$ calcd. for $C_{20}H_{19}FN_3O_4$: 384.1354, found: 384.1364.

***6-(2-Morpholinoacetamido)-3-oxo-2-(4-(trifluoromethoxy) phenyl)-3H-indole 1-oxide 14*:** Orange solid, yield: 52%, mp: 103-104°C. ^{1}H NMR (300 MHz, $CDCl_3$): δ: 9.57 (s, 1H, NH), 8.81-8.76 (m, 2H), 7.92-7.85 (m, 2H), 7.64 (dd, *J*=8.0, 0.4 Hz, 1H), 7.35 (ddt, *J*=8.1, 2.1, 1.0 Hz, 2H), 3.85-3.82 (m, 4H), 3.23 (s, 2H), 2.70-2.67 (m, 4H). ^{13}C NMR (70 MHz, $CDCl_3$): δ: 185.5, 168.5, 149.4, 143.8, 131.7, 129.7 (2C), 124.4, 123.3, 122.1, 120.6 (2 C), 120.2, 118.6, 117.7, 105.6, 67.0 (2 C), 62.4, 53.8 (2 C). IR (KBr, cm^{-1}): 3417, 3263, 1707, 1639, 1531, 1501, 1425, 1377, 1256, 1155, 1115, 1015, 845. MS-(+ESI), *m/z*: 450 [M + H]$^+$, 899 [2M + H]$^+$. ESI-HRMS [M + H]$^+$ calcd. for $C_{21}H_{19}F_3N_3O_5$: 450.1271, found: 450.1272.

***2-(4-Fluorophenyl)-3-oxo-6-(2-(piperidin-1-yl)acetamido)-3H-indole 1-oxide 15*:** Orange solid, yield: 65%, mp: 172-174°C. ^{1}H NMR (300 MHz, $CDCl_3$): δ: 9.81 (s, 1H, NH), 8.80-8.73 (m, 2H), 7.88-7.85 (m, 2H), 7.62-7.59 (m, 1H), 7.24-7.16 (m, 2H), 3.14 (s, 2H), 2.61-2.57 (m, 4H), 1.73-1.66 (p, *J*=5.7 Hz, 6H). ^{13}C NMR (70 MHz, $CDCl_3$): δ: 185.7, 169.6, 165.3, 162.0, 149.4, 144.1, 130.3, 123.2 (2 C), 122.4, 119.8, 117.5, 115.9 (2C), 105.4, 62.7, 55.0 (2C), 26.3 (2C), 23.5. IR (KBr, cm^{-1}): 3413, 3278, 2934, 1705, 1643, 1500, 1422, 1373, 1295, 1249, 1155, 1133, 1104, 843. MS-(-APCI), *m/z*: 254, 282, 311, 380 [M^{-}], 426. ESI-HRMS [M + H]$^+$ calcd. for $C_{21}H_{21}FN_3O_3$: 382.1561, found: 382.1574.

***3-Oxo-6-(2-(piperidin-1-yl)acetamido)-2-(4-(trifluoromethoxy) phenyl)-3H-indole 1-oxide 16*:** Red solid, yield 54%, mp: 161-163°C. ^{1}H NMR (300 MHz, $CDCl_3$): δ: 9.83 (s, 1H, NH), 8.81-8.76 (m, 2H), 7.90-7.84 (m, 2H), 7.63-7.60 (m, 1H), 7.34-7.32 (m, 2H), 3.14 (s, 2H), 2.59 (t, *J*=5.3 Hz, 4H), 1.70 (p, *J*=5.6 Hz, 6H). ^{13}C NMR (70 MHz, $CDCl_3$): δ: 185.5, 169.6, 150.3, 144.1, 131.6, 129.6 (2 C), 124.5, 123.3, 122.1, 120.5, 120.0 (2 C), 118.6, 117.5, 105.5, 62.7, 55.0 (2 C), 26.3 (2 C), 23.5. IR (KBr, cm^{-1}): 3423, 3229, 2940, 1725, 1604, 1535, 1423, 1376, 1348, 1299, 1278, 1250, 1208, 1156, 865, 844. MS-(-APCI), *m/z*: 446 [M^{-}], 492. ESI-HRMS [M + H]$^+$ calcd. for $C_{22}H_{21}F_3N_3O_4$: 448.1479, found: 448.1490.

***2-(4-Chlorophenyl)-6-(2-morpholinoethoxy)-3-oxo-3H-indole 1-oxide 17*:** Orange solid, yield: 86%, mp: 137-139°C. ^{1}H NMR (300 MHz, $CDCl_3$): δ: 8.72-8.67 (m, 2H), 7.58 (d, *J*=8.1 Hz, 1H), 7.51-7.46 (m, 2H), 7.27 (d, *J*=2.1 Hz, 1H), 6.97 (dd, *J*=8.1, 2.2 Hz, 1H), 4.27 (t, *J*=5.6 Hz, 2H), 3.78- 3.75 (m, 4H), 2.87 (t, *J*=5.6 Hz, 2H), 2.63-2.60 (m, 4H). ^{13}C NMR (70 MHz, $CDCl_3$): δ: 185.5, 164.8, 150.5, 136.7, 131.9, 129.1 (2C), 128.9 (2C), 124.5, 123.6, 115.9, 115.1, 101.9, 67.2, 66.9 (2C), 57.2, 54.1 (2C). IR (KBr, cm^{-1}): 1708, 1641, 1616, 1519, 1379, 1235, 1113, 1069, 825. MS-(+ESI), *m/z*: 387 [M + H]$^+$. ESI-HRMS [M + H]$^+$ calcd. for $C_{20}H_{20}ClN_2O_4$: 387.1106, found: 387.1117.

***2-(4-Chlorophenyl)-6-(2-morpholinoacetoxy)-3-oxo-3H-indole 1-oxide 18*:** Red solid, yield: 72%, mp: 229-231°C. ^{1}H NMR (300 MHz, C_3D_6O): δ: 8.74-8.63 (m, 2H), 7.60-7.58 (m, 1H), 7.57-7.50 (m, 2H), 7.16 (dd, *J*=2.1, 0.4 Hz, 1H), 7.03 (dd, *J*=8.0, 2.1 Hz, 1H), 3.85-3.82 (m, 4H), 3.04 (s, 2H), 2.68-2.67 (m, 4H). ^{13}C NMR (70 MHz, C_3D_6O): δ: 185.2, 167.0, 164.2, 150.8, 149.8, 135.5, 128.9 (2 C), 128.5 (2C), 125.4, 123.7, 116.7, 114.2, 102.5, 66.9 (2 C), 58.1, 54.2 (2 C). IR (KBr, cm^{-1}): 3436, 1702, 1686, 1653, 1584, 1519, 1492, 1373, 1260, 1179, 1093, 1009, 862, 832. MS-(-APCI), *m/z*: 272 [M - $C_6H_{10}NO_2$]$^{-}$, 545. ESI-HRMS [M - $C_6H_{10}NO_2$ + H]$^+$ calcd. for $C_{14}H_9ClNO_3$: 274.0265, found: 274.0272.

***2-(4-Chlorophenyl)-6-(2-morpholinoacetamido)-3-oxo-3H-indole 1-oxide 19*:** Orange solid, yield: 65%, mp: 201-203°C. ^{1}H NMR (300 MHz, $CDCl_3$): δ: 9.56 (s, 1H, NH), 8.71-8.66 (m, 2H), 7.89-7.84 (m, 2H), 7.63-761 (m, 1H), 7.50-7.46 (m, 2H), 3.85-3.82 (m, 4H), 3.22 (s, 2H), 2.69-2.66 (m, 4H). ^{13}C NMR (70 MHz, $CDCl_3$): δ: 185.5, 168.5, 149.4, 143.7, 136.7, 131.9, 129.1 (2C), 128.9 (2C), 124.4, 123.2, 120.1, 117.8, 105.5, 67.0 (2 C), 62.4, 53.8 (2 C). IR (KBr, cm^{-1}): 3415, 3246, 1713, 1643, 1515, 1499, 1378, 1253, 1110, 1011, 837. MS-(+ESI), *m/z*: 400 [M + H]$^+$, 799 [2M + H]$^+$. ESI-HRMS [M + H]$^+$ calcd. for $C_{20}H_{19}ClN_3O_4$: 400.1059, found: 400.1068.

***2-(4-Chlorophenyl)-3-oxo-6-(2-(piperidin-1-yl)acetamido)-3H-indole 1-oxide 20*:** Red solid, yield: 56%, mp: 176-178°C. ^{1}H NMR (300 MHz, $CDCl_3$): δ: 9.81 (s, 1H, NH), 8.71-8.66 (m, 2H), 7.87-7.84 (m, 2H), 7.62-7.59 (m, 1H), 7.50-7.45 (m, 2H), 3.14 (s, 2H), 2.61-2.57 (m, 4H), 1.73-1.66 (m, 6H). ^{13}C NMR (70 MHz, $CDCl_3$): δ: 185.6, 169.6, 149.4, 144.1, 136.6, 131.9, 129.1 (2 C), 128.9 (2C), 124.5, 123.2, 119.9, 117.5, 105.5, 62.7, 55.0 (2C), 26.3 (2C), 23.5. IR (KBr, cm^{-1}): 3477, 3414, 3232, 2943, 1709, 1643, 1504, 1421, 1383, 1243, 1112, 1013, 846, 820. MS-(-APCI), *m/z*: 396 [M^{-}], 442. ESI-HRMS [M + H]$^+$ calcd. for $C_{21}H_{21}ClN_3O_3$: 398.1266, found: 398.1280.

Crystallography

The single crystal of compound **14** was obtained in *m*-xylene solution. Data were collected at low temperature (100 K) on a Bruker Kappa Apex II diffractometer using a Mo-Kα radiation (λ=0.71073 Å) micro-source equipped with an Oxford Cryosystems Cryostream Cooler Device. The structure was solved by Direct Methods using SHELXS97 [16] and refined by means of least-squares procedures using Crystal software package [17]. The Atomic Scattering Factors were taken from International tables for X-Ray Crystallography [18]. All hydrogen atoms were placed geometrically and refined using a riding model. All non-hydrogen atoms were anisotropically refined. Molecule drawings were performed with the ORTEP 32 program [19] with 30% probability displacement ellipsoids for non-hydrogen atoms. The crystal structures have been deposited at the Cambridge Crystallographic Data Centre and allocated the deposition number: CCDC 1557289.

Crystal data: $C_{21}H_{18}F_3N_3O_5$, H_2O, M=467.40, colorless needle crystal, 0.12 × 0.04 × 0.02 mm, triclinic, space group *P*-1, a=7.392(2), b=9.743(3), c=15.089(5) Å, α=103.336 (13), β=92.655 (13), γ=105.701 (13)°, *V*=1011.1 (5) Å^3, Z=2, d=1.535, μ(MoKα)=0.71073 Å, 310 parameters, 38,563 reflexions measured, 4,850 unique (R_{int}=0.050), 3,480 reflections used in the calculations (I>2.0 σ[I]), R=0.041, *w*R=0.047, residual electronic density=-0.51/0.68 (e.Å^{-3}).

Biology

In vitro Plasmodium falciparum **culture and parasite growth inhibition assays:** The FcB1 strain of *P. falciparum* (chloroquine-resistant strain) was maintained in RPMI 1640 medium and 5% human serum (EFS, Toulouse, France). Human RBCs (group O ±, Toulouse,

France) were extensively washed with cold RPMI medium to remove remaining plasma and leukocytes. Parasitized RBCs were maintained in 25 cm^2 culture flasks in a controlled atmosphere and synchronized by D-sorbitol lysis. As control, stock solution of chloroquine (CQ, Sigma (refC6628) was dissolved in culture medium (stock solution: 1 mg/mL). For the drug assays, serial drug dilutions in triplicates (100 µL/well) were made in RPMI medium (final concentration of DMSO is 0.5%) and were added to a *P. falciparum* culture media (2% hematocrit, 1% parasitemia, 100 µL/well) in a 96-well culture plate. 48 h after the beginning of incubation, plates were washed three times with 150 µL of PBS and 100 µl of a lysis buffer containing 2 × SG (sybr green) I was added to 100 µL of each dilution of the parasitized RBCs + drugs in a black 96-well plate and incubated in the dark at room temperature for 2 h. Subsequently, the fluorescence values were determined using a fluorescence plate reader at 485 nm and 518 nm excitation and emission wavelengths, respectively. The fluorescence (after subtraction of the background fluorescence for nonparasitized RBCs) values were plotted, and the IC_{50} values were determined by linear regression analysis.

***In vitro* cytotoxicity assay: cytotoxicity against the Vero cell line:** The evaluation of the tested molecules cytotoxicity by MTT assay on the Vero cell line was performed according to the following protocol: in brief, cells (1×10^4 cells/mL) in 100 µL of complete medium, (MEM supplemented with 10% fetal calf serum (FCS), 2 mM l-glutamine and NEAA 1X) were seeded into each well of 96-well plates and incubated at 37°C and 5% CO_2. After 24 h incubation, 100 µL of medium with various product concentrations and appropriate controls (DMSO) were added, and the plates were incubated for 72 h at 37°C and 5% CO_2. Each plate-well was then microscope-examined to detect possible precipitate formation before the medium was pipetted from the wells. 100 µL of MTT solution (0.5 mg/mL in MEM) were then added to each well. Cells were incubated for 2 h at 37°C and 5% CO_2. The MTT solution was then removed, and DMSO (100 µL/well) was added to dissolve the resulting formazan crystals. Plates were shaken vigorously (300 rpm) for 5 min. The absorbance was measured at 570 nm with a microplate spectrophotometer (Eon BioTek). CC_{50} were calculated by non-linear regression analysis processed on dose-response curves, using GraphPad Prism® V7 software. CC_{50} values represent the mean value calculated from three independent experiments.

Selectivity index (SI): The selectivity indices presented correspond to the ratios between, respectively, the toxicity on Vero cell line (or MCF-7 line) and the FcB1 antiplasmodial activity. They are calculated as follows: SI=CC_{50} (Vero)/IC_{50} (FcB1).

Results and Discussion

Chemistry

The synthetic pathway for 6-amino-2-arylindolone-*N*-oxides **9-20** is illustrated in Schemes 1 and 2. *O*-Alkylation of 4-iodo-3-nitrophenol **a** with 1,2-dibromoethane in refluxing ethanol, in the presence of K_2CO_3, produced the bromo ether **c** [20]. Treatment of bromoacetyl bromide with 4-iodo-3-nitrophenol **a** or 4-iodo-3-nitrophenylamine **b** in dichloromethane at -78°C, in the presence of triethylamine, produced the bromo ester and the bromo amide **d** and **e**, respectively [21]. The NaI mediated reaction of bromo intermediates **c**-**e** gave the tertiary amino compounds **f**-**i** after treatment with morpholine or piperidine in the presence of K_2CO_3 as a base [20]. The synthesis of the indolone-*N*-oxide derivatives **9-20** is divided into two sub-steps following a previously reported method [22,23].

The log P_{calc} values [24] (Table 1) range between 2.08 and 3.05, and compounds **10** and **16** are the most lipophilic. Compounds are soluble in water in the range 44-183 µM. Morpholino-*amide*-INODs **13**, **14** and **19** have the best water solubility (183, 156 and 175 µM, respectively).

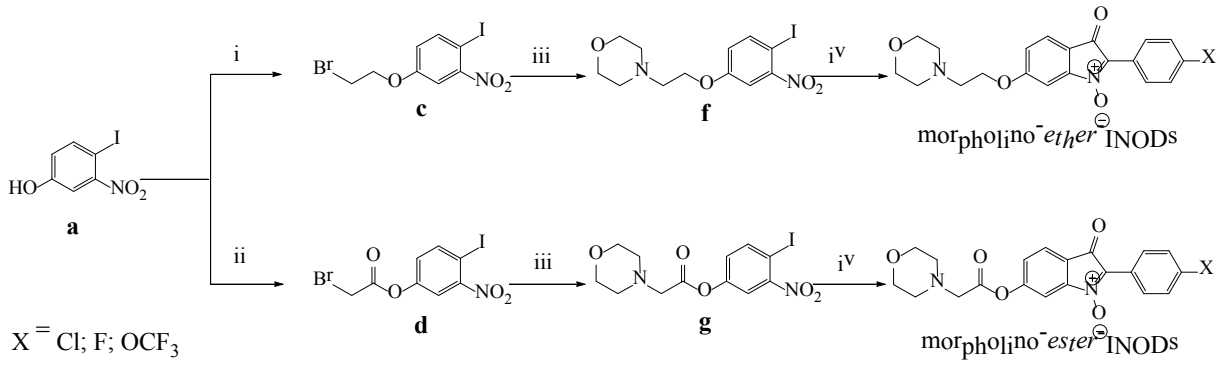

Scheme 1: Reagents and conditions: (i) 1,2-dibromoethane, K_2CO_3, ethanol reflux; (ii) bromoacetyl bromide, Et_3N, DCM, - 78°C; (iii) 1. NaI, acetonitrile reflux; 2. morpholine, K_2CO_3, reflux; (iv) 1. Alkyne, $Pd(PPh_3)_2Cl_2$, CuI, Et_3N, N_2, rt; 2. $Pd(CH_3CN)_2Cl_2$, CH_3CN, N_2, reflux 86°C.

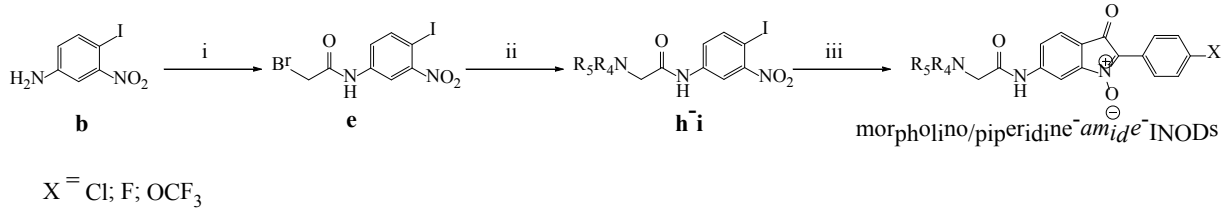

Scheme 2: Reagents and conditions: (i) bromoacetyl bromide, Et_3N, DCM, -78°C; (ii) 1. NaI, acetonitrile reflux; 2. R_4R_5NH, K_2CO_3, reflux; (iii) 1. Alkyne, $Pd(PPh_3)_2Cl_2$, CuI, Et_3N, N_2, rt; 2. $Pd(CH_3CN)_2Cl_2$, CH_3CN, N_2, reflux 86°C.

Compound	Structure	Log P_{calc} [b] (VCCLAB)	IC_{50} (nM) with FcB1 strain	Solubility in water (µM)	Selectivity index
1[a]	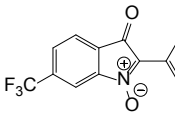	1.96	889	ND	21.9[c]
2[a]	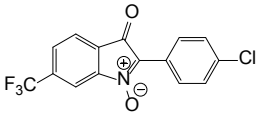	3.26	186	ND	16.6[c]
3[a]	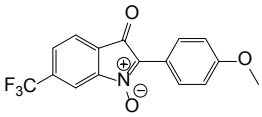	2.72	135	ND	58.5[c]
4[a]	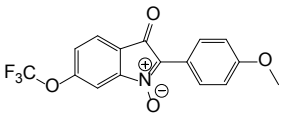	2.88	133	ND	87.9[c]
5[a]	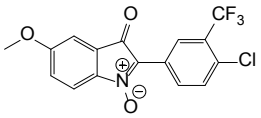	3.32	50	ND	270[c]
6[a]	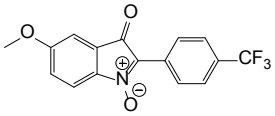	2.74	43	ND	272[c]
7[a]	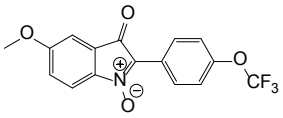	2.90	20	ND	415[c]
8[a]	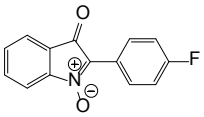	2.06	120	ND	72.5[c]
9	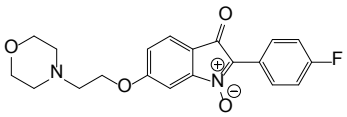	2.44	45.9	135	>294.1[d]
10	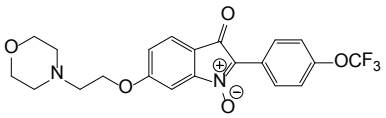	3.05	41.3	115	>278.4[d]
11	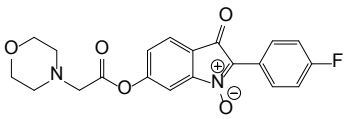	2.30	52.0	52	>250[d]
12	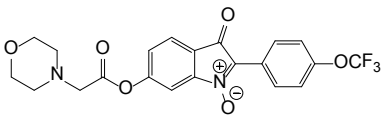	2.86	42.9	44	>128[d]
13	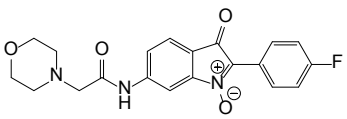	2.08	39.1	183	>335[d]

14	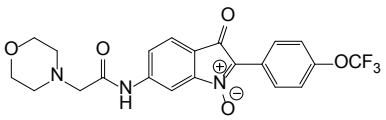	2.74	15.5	156	>716.1[d]
15	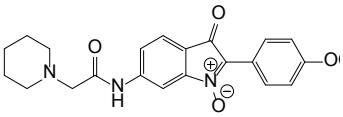	2.66	26.24	157	>499[d]
16	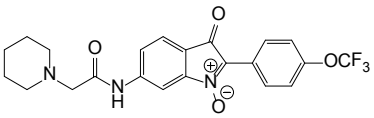	3.05	61.5	134	>182.1[d]
17	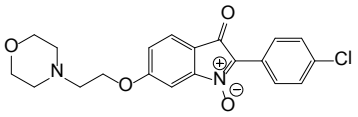	2.60	72.5	129	>177.9[d]
18	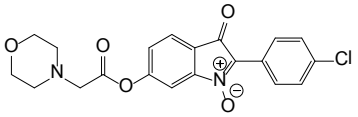	2.48	75.0	50	>166.6[d]
19	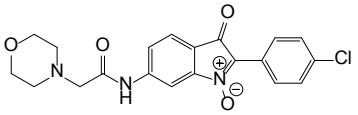	2.35	75.2	175	>166.2[d]
20	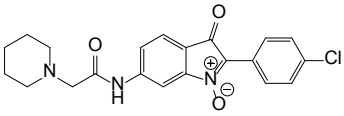	2.93	58.7	151	214.6[d]
	Chloroquine	5.28	151 ± 6		167
	Sodium artesunate	2.29	6 ± 3		1 633

[a]Ref [8]; [b]Log P_{calc} calculated with VCCLAB (http://www.virtuallaboratory.org/lab/alogps/start.html); [c]Selectivity index (MCF-7/FcB1); [d]Selectivity index (Vero/FcB1); ND, not determined.

Table 1: Structure of indolone-*N*-oxides and *in vitro* antiplasmodial and cytotoxic activities.

The compounds were chemically characterized by thin-layer chromatography (TLC) and high-performance liquid chromatography (HPLC), infrared (IR), nuclear magnetic resonance (NMR) (^{1}H and ^{13}C) and mass spectrometry, including high-resolution mass spectrometry (HRMS). The structure of **14**, 2-(4-trifluoromethoxy)phenylindolone-*N*-oxide, was also established by X-ray crystallographic analysis (Figure 2). In **14**, the indolone-*N*-oxide ring and the 4-trifluoromethoxyphenyl ring are almost co-planar, the dihedral angle between the two rings systems being (N1-C2-C10-C11: 14.5°) (Figure 2).

Biology

The series was evaluated for antiplasmodial activity against the *P. falciparum* FcB1 through *in vitro* red blood cell-based culture using a SYBR-Green-I assay. A summary of these assay results is presented in Table 1. New fluorinated indolone-*N*-oxides were active against *P. falciparum* FcB1 with IC_{50} values of <75 nM. The non-substituted compound **1** (2-phenylindolone-*N*-oxide; R^1=R^2=R^3=H) had the lowest antiplasmodial activity (IC_{50}=889 nM). Replacement of R^2 (H) by a trifluoromethyl or trifluoromethoxy group improved the activity (IC_{50}: **2**=186 nM, **3**=135 nM, **4**=133 nM). Replacement of R^3 (H) by a trifluoromethyl, trifluoromethoxy or fluoro group conferred good activity (IC_{50}: **5**=50 nM, **6**=43 nM, **7**=20 nM, **8**=120 nM). In compounds **9**-**16**, the introduction of morpholino or piperidinyl group at R^2 (the amino groups were linked to different INODs via ether, ester or amide linkage) and a fluoro or trifluoromethoxy group at R^3 led to the best antiplasmodial activities in this series with IC_{50} values ranging from 15.5 to 61.5 nM. Activity decreased when the fluoro group was replaced by a chloro group (compounds **9**, **11**, **13** and **15** versus **17**, **18**, **19** and **20**, respectively). Compounds with amino-amide-INOD structures (the amino groups being morpholino or piperidine) were found to be more active than their ether and ester linked counterparts (IC_{50}: **13**=39.1 nM, **14**=15.5 nM, **15**=26.2 nM). The morpholino-linker-INODs (compounds **13**, **14**, and **19**) and the piperidine-linker-INODs (compounds **15**, **16**, and **20**) exhibited almost identical activity against *P. falciparum* FcB1, which indicates that the morpholino and piperidine amino groups do not have a notable impact on the antiplasmodial activity.

All the synthesized compounds were further evaluated by MTT assay for cytotoxicity against MCF7 or Vero cell lines (Table 1). All the compounds evaluated showed good selectivity index in the range of 16-720. Compounds **9**-**20** were the most potent against malarial parasites and also exhibited high selectivity index in the range of 177-720.

Conclusion

In summary, in this study a series of amino-linker-INODs were

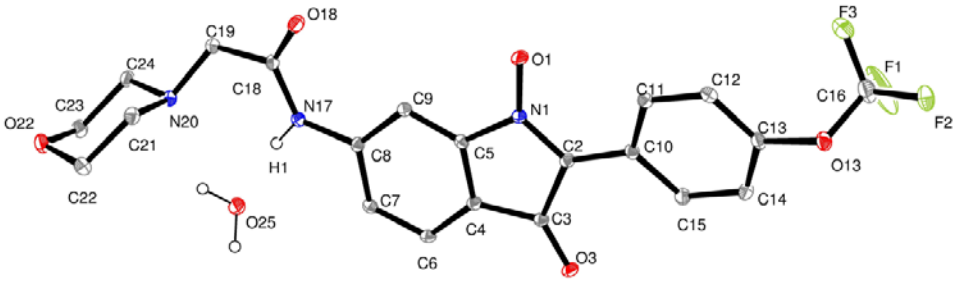

Figure 2: Molecular structure of **14** crystallized with one water molecule. Hydrogen atoms on the skeletons were omitted for clarity. Selected bond lengths and angles are presented in Table S1 in the Supporting Information.

synthesized and evaluated for their antimalarial activity. The *in vitro* evaluation of these compounds against *P. falciparum* FcB1 displayed activity in the nM range. Fluorinated amino-INODs **9-16** exhibited very good antiplasmodial activity and low toxicity against the Vero cell lines. In addition, these fluorinated-INODs exhibited high selectivity indices.

References

1. Ojima I (2009) Fluorine in Medicinal Chemistry and Chemical Biology. John Wiley & Sons, Chichester, UK, p: 640.
2. Muller K, Faeh C, Diederich F (2007) Fluorine in pharmaceuticals: Looking Beyond Intuition. Science 317: 1881-1886.
3. Begue JP, Bonnet-Delpon D (2006) Recent advances (1995-2005) in fluorinated pharmaceuticals based on natural products. J Fluorine Chem 127: 992-1012.
4. Isanbor C, O'Hagan D (2006) Fluorine in medicinal chemistry: A review of anti-cancer agents. J Fluorine Chem 127: 303-319.
5. Cottet F, Marull M, Lefebvre O, Schlosser M (2003) Recommendable Routes to Trifluoromethyl-Substituted Pyridine- and Quinolinecarboxylic Acids. Eur J Org Chem 2003: 1559-1568.
6. Zhou Y, Wang J, Gu Z, Wang S, Zhu W, et al. (2016) Next generation of fluorine-containing pharmaceuticals, compounds currently in phase II-III clinical trials of major pharmaceutical companies: New structural trends and therapeutic areas. Chem Rev 116: 422-518.
7. Gillis EP, Eastman KJ, Hill MD, Donnelly DJ, Meanwell NA (2015) Applications of fluorine in medicinal chemistry. J Med Chem 58: 8315-8359.
8. Nepveu F, Kim S, Boyer J, Chatriant O, Ibrahim H, et al. (2010) Synthesis and antiplasmodial activity of new indolone-N-oxide derivatives. J Med Chem 53: 699-714.
9. Ibrahim H, Pantaleo A, Turrini F, Arese P, Nallet JP, et al. (2011) Pharmacological properties of indolone-N-oxides controlled by a bioreductive transformation in red blood cells. Med Chem Comm 2: 860-869.
10. Nepveu F, Najahi E, Valentin A (2014) Antimalarial activities of indolones and derivatives. Curr Top Med Chem 14: 1643-1652.
11. Reybier K, Thi HYN, Ibrahim H, Perio P, Montrose A, et al. (2012) Electrochemical behavior of indolone-N-oxides: relationship to structure and antiplasmodial activity. Bioelectrochem 88: 57-64.
12. Thi HYN, Ibrahim H, Reybier K, Perio P, Souard F, et al. (2013) Pro-oxidant properties of indolone-N-oxides in relation to their antimalarial properties. J Inorg Biochem 126: 7-16.
13. Cassagnes LE, Rakotoarivelo N, Sirigu S, Pério P, Najahi E, et al. (2017) Molecules 22: 1-16.
14. Pantaleo A, Ferru E, Vono R, Girbaldi G, Lobina O, et al. (2012) New antimalarial indolone-N-oxides, generating radical species, destabilize the host cell membrane at early stages of Plasmodium falciparum growth: role of band 3 tyrosine phosphorylation. Free Rad Bio Med 52: 527-536.
15. Ibrahim N, Ibrahim H, Dormoi J, Briolant S, Pradines B, et al. (2014) Albumin-bound nanoparticles of practically water-insoluble antimalarial lead greatly enhance its efficacy. Int J Pharm 64: 214-224.
16. SHELX97 (Includes SHELXS97, SHELXL97, CIFTAB) (1998) Programs for Crystal Structure Analysis (Release 97-2). Sheldrick GM, Institüt für Anorganische Chemie der Universität, Tammanstrasse 4, D-3400 Göttingen, Germany.
17. Betteridge PW, Carruthers JR, Cooper RI, Prout K, Watkin DJ (2003) CRYSTALS Version 12: Software for guided crystal structure analysis. Journal of Applied Crystallography 36: 1487.
18. Schmitz W (1975) International Tables for X-ray Crystallography, vol. IV (Ergänzungsband). Herausgegeben von der International Union of Crystallography. The Kynoch Press, Birmingham, England, 1974, 366 Seiten einschließlich Tabellen und Sachwortverzeichnis. Crystal Research and Technology 10: K120.
19. Farrugia LJ (1997) ORTEP3 for Windows. J Appl Crystallogr 30: 565.
20. Chen X, Sassano MF, Zheng LY, Setola V, Chen M, et al. (2012) Structure-functional selectivity relationship studies of beta-arrestin-biased dopamine D-2 receptor agonists. J Med Chem 55: 7141-7153.
21. Lepri S, Buonerba F, Goracci L, Velilla L, Ruzziconi R, et al. (2016) Indole based weapons to fight antibiotic resistance: A structure-activity relationship study. J Med Chem 59: 867-891.
22. Najahi E, Rakotoarivelo NV, Valentin Nepveu AF (2014) Amino derivatives of indolone-N-oxide: Preparation and antiplasmodial properties. Eur J Med Chem 76: 369-375.
23. Ramana CV, Patel P, Vanka K, Miao B, Degterev A (2010) A combined experimental and density functional theory study on the Pd-mediated cycloisomerization of o-alkynylnitrobenzenes-synthesis of isatogens and their evaluation as modulators of ROS-mediated cell death. Eur J Org Chem 2010: 5955-5966.
24. Virtual Computational Chemistry Laboratory (2009) ALOGPS 2.1. Available from: http://www.virtuallaboratory.org/lab/alogps/ Accessed on: July 11, 2009.